Push-pull 1,3-thiazolium-5-thiolates. Formation *via* concerted and stepwise pathways, and theoretical evaluation of NLO properties†,‡

David Cantillo,*[a] Martín Ávalos,[a] Reyes Babiano,[a] Pedro Cintas,[a] José L. Jiménez,[a] Mark E. Light,[b] Juan C. Palacios[a] and Valentín Rodríguez[a]

Received 12th July 2010, Accepted 23rd August 2010
DOI: 10.1039/c0ob00416b

The transformation of münchnones (mesoionic rings featuring the 1,3-oxazolium-5-olate core) into their sulfur counterparts (1,3-thiazolium-5-thiolates) by reaction with CS_2, pioneered by Huisgen and his group in the early 1970s, has been re-investigated in detail by means of both experimental and theoretical methods. The synthetic strategy can be tuned to incorporate donor and acceptor groups in appropriate positions. Calculations of molecular hyperpolarizabilities together with orbital topologies evidence that these sulfur-containing heterocycles exhibit nonlinear optical responses, thereby pointing to potential applications of mesoionic structures in the NLO field. From a mechanistic viewpoint, modeling of the whole systems at the B3LYP/6-31G(d) level reveals that concerted and stepwise pathways are operative depending on the substitution pattern of the parent münchnone, which also account for the experimental results.

Introduction

Thionation of mesoionic rings represents a valuable strategy to incorporate a bulkier and more polarizable atom in such five-membered aromatic heterocycles. The transformation of 1,3-oxazolium-5-olate systems (münchnones) into 1,3-thiazolium-5-thiolates by reaction with carbon disulfide was first described by Huisgen and associates more than four decades ago,[1] and since then it has been recognized as a model for the synthesis of mesoionic heterocycles based on tandem cycloaddition–retrocycloaddition processes.[2] The last decade has witnessed a renaissance of these protocols because they can be applied with excellent results to the preparation of various mesoionic systems with potential non-linear optical properties.[3] We have also used recently a related methodology to obtain 1,3-thiazolium-4-thiolates by reaction of thioisomünchnones with aryl isothiocyanates,[4] and finding that a stepwise thionation competes, often favorably, with the expected cycloaddition–retrocycloaddition reaction.[5]

In this paper we report a thorough experimental and theoretical study aimed at designing a series of push-pull 1,3-thiazolium-5-thiolates from the corresponding münchnones and carbon disulfide. Mechanistic investigations have been performed by DFT calculations at the B3LYP/6-31G(d) level. Further assessing of second-order hyperpolarizabilities unveils the potentiality of such substances in the field of nonlinear optics.

Results and Discussion

Synthesis and Structure Elucidation

According to the described procedure,[6] 1,3-oxazolium-5-olates can be synthesized by a three-sequence protocol. The first is actually a multicomponent process in which the iminium ion (**5–7**) formed by addition–elimination reaction of an aromatic aldehyde (**1–3**) with an alkylammonium halide (**4**), undergoes *in situ* nucleophilic addition of cyanide ion to give an aminonitrile (**8–10**) that is subsequently hydrolyzed in acidic solution. The application of this methodology to benzaldehyde, *p*-anisaldehyde, and 4-fluorobenzaldehyde allowed us to obtain the corresponding *C*-aryl-*N*-methylglycine hydrochlorides **11–13** (Scheme 1).

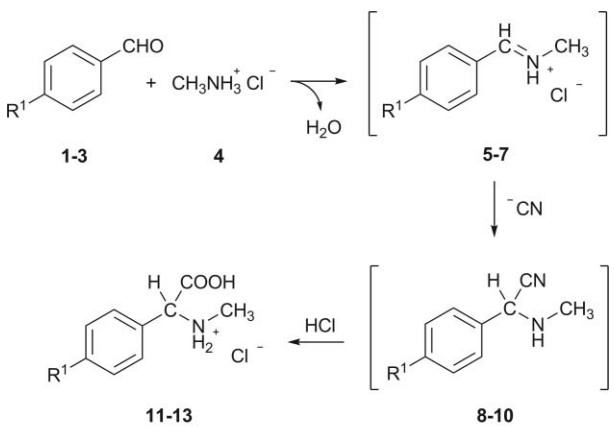

Scheme 1

[a]*Departamento de Química Orgánica e Inorgánica, QUOREX Research Group, Facultad de Ciencias, Universidad de Extremadura, E-06006, Badajoz, Spain. E-mail: dcannie@unex.es*
[b]*Department of Chemistry, University of Southampton, Highfield, Southampton, UK, SO17 1BJ*

† Dedicated to Prof. José Fuentes Mota

‡ Electronic supplementary information (ESI) available: Copies of NMR spectra for all new compounds, UV spectra and cyclic voltammograms for 1,3-thiazolium-5-thiolate systems, complete Cartesian coordinates and energies for all calculated structures, crystal data for compounds **14**, **15** and **18** data in CIF format, and crystal structure simulation outputs in PDB format. CCDC reference numbers 784450–784452. For ESI and crystallographic data in CIF or other electronic format see DOI: 10.1039/c0ob00416b

Since *p*-nitrobenzaldehyde did not react under the above conditions, the synthesis of *N*-methyl-*C*-(4-nitrophenyl)glycine (**14**) was attempted by conventional nitration of **11** in following the operational procedure described previously.[6] Remarkably, both ^{1}H and ^{13}C NMR data are consistent with the exclusive formation of *N*-methyl-*C*-(3-nitrophenyl)glycine (**15**), thereby evidencing a different orientation of the nitro group. *N*-Acylation of **12** with 4-nitrobenzoyl and 4-fluorobenzoyl chlorides led to the formation of *N*-acyl-*C*-aryl-*N*-methylglycines, **16** and **17** respectively, while treatment of **13** and **15** with *p*-anisoyl chloride gave rise to the *N*-acyl derivatives **18** and **19**.

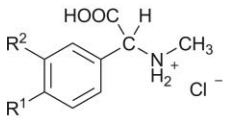

14 $R^1 = NO_2$; $R^2 = H$
15 $R^1 = H$; $R^2 = NO_2$

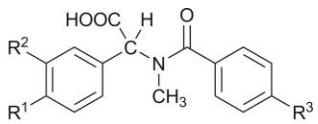

16 $R^1 = OCH_3$; $R^2 = H$; $R^3 = NO_2$
17 $R^1 = OCH_3$; $R^2 = H$; $R^3 = F$
18 $R^1 = F$; $R^2 = H$; $R^3 = OCH_3$
19 $R^1 = H$; $R^2 = NO_2$; $R^3 = OCH_3$

Cyclodehydration of the *N*-acyl-*C*-aryl-*N*-methylglycines **16–19** was conducted with acetic anhydride under argon at temperatures below 55 °C yielding the corresponding 2,4-diaryl-3-methyl-1,3-oxazolium-5-olates **20–23**. These substances must be used immediately as substrates to avoid further decomposition, which takes place rapidly in solution or progressively (several days) when stored under vacuum. From a strategic standpoint, the first two synthetic stages enable the combination of aryl groups in positions 2 and 4 of the heterocycle en route to different push-pull systems.

Finally, the preparation of 2,4-diaryl-3-methyl-1,3-thiazolium-5-thiolates **24–28** (Scheme 2, Table 1) was carried out by refluxing a mixture of **20–23** and excess of carbon disulfide in *N*,*N*-dimethylformamide (DMF) solution, until observing the disappearance of the parent mesoionic (TLC monitoring).

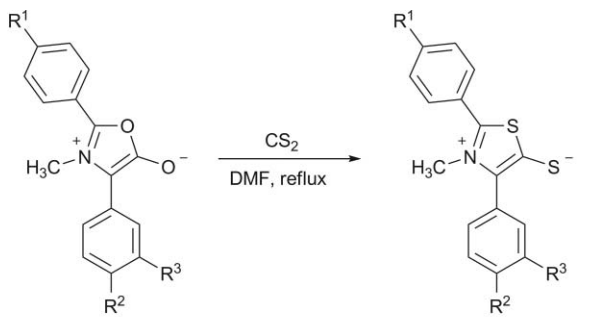

20 $R^1 = NO_2$; $R^2 = OCH_3$; $R^3 = H$
21 $R^1 = F$; $R^2 = OCH_3$; $R^3 = H$
22 $R^1 = OCH_3$; $R^2 = F$; $R^3 = H$
23 $R^1 = OCH_3$; $R^2 = H$; $R^3 = NO_2$

24 $R^1 = NO_2$; $R^2 = OCH_3$; $R^3 = H$
25 $R^1 = OCH_3$; $R^2 = NO_2$; $R^3 = H$
26 $R^1 = F$; $R^2 = OCH_3$; $R^3 = H$
27 $R^1 = OCH_3$; $R^2 = F$; $R^3 = H$
28 $R^1 = OCH_3$; $R^2 = H$; $R^3 = NO_2$

Scheme 2

While compound **27** could easily be isolated by spontaneous crystallization after 1 h-heating, **24**, **25**, **26** and **28** required longer reaction times (~4 h) and had to be purified by column chromatography (benzene–acetonitrile gradient). When compound **20** was used as starting material, two products (**24** and **25**) were formed in a 1 : 1.25 ratio, whose structures could be unequivocally assigned by single-crystal X-ray diffraction (Fig. 1). Compound

Table 1 Reaction of münchnones **20–23** with carbon disulfide in DMF at reflux

Substrate	Time/h	Product (yield%)
20	4	**24** (34) + **25** (43)
21	4	**26** (61)
22	1	**27** (98)
23	4	**28** (36)

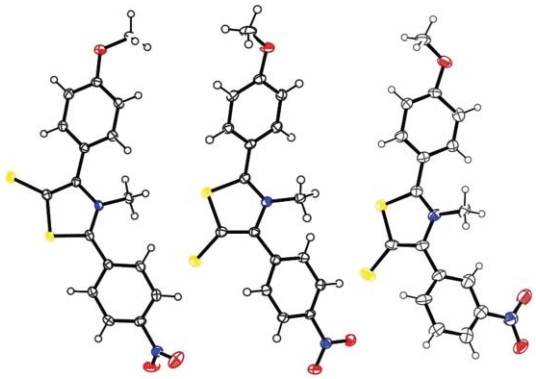

Fig. 1 ORTEP diagrams of the crystal structures of **24**, **25** and **28**.

24 has been previously described,[3d] as the only regioisomer of the cycloaddition reaction; however this process does actually yield two products as outlined herein.

It is noteworthy the different arrangements adopted by the nitro group in the molecular structure of compounds **24** and **25**. While in **25** that group is coplanar with the aromatic ring (O–N–C–C dihedral angle: 2.9°), the disposition in **24** significantly deviates from coplanarity (O–N–C–C dihedral angle: 40.5°).

To rationalize that unexpected inhibition to resonance, we have also simulated computationally (at the B3LYP/6-31G(d), using the GAUSSIAN03[7] package) the crystal lattice of **25** in which two 4-nitrophenyl groups of vicinal molecules interact each other. On the basis of crystal data as well, we have also incorporated the six surrounding molecules possessing a close atom (as sum of van der Waals radii) to either nitro group of the two above-mentioned vicinal molecules. This protocol gives rise to a whole system comprising 8 molecules and 304 atoms (Fig. 2).

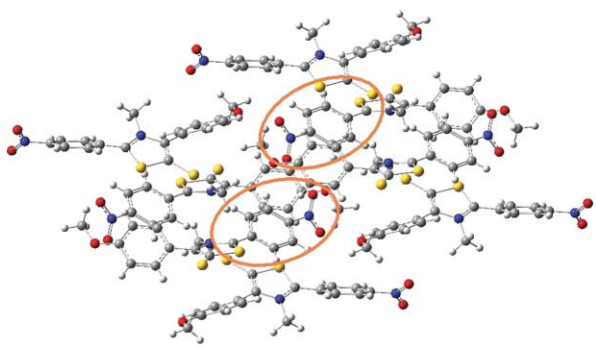

Fig. 2 Crystal structure simulation.

Single-point energy calculations revealed that the supramolecular structure is more stable, by 6.7 kcal mol^{-1}, than an analogous one for which both nitro groups are coplanar to phenyl rings. NBO

calculations ruled out intermolecular donor–acceptor interactions as responsible of the energy difference. Therefore, the origin of such a stabilizing effect should presumably be ascribed to electrostatic interactions involving the oxygen atoms of nitro groups with other oxygen atoms present in contiguous nitro and methoxy groups (Fig. 3a), which decrease as the 4-nitrophenyl groups deviate from coplanarity (Fig. 3b).

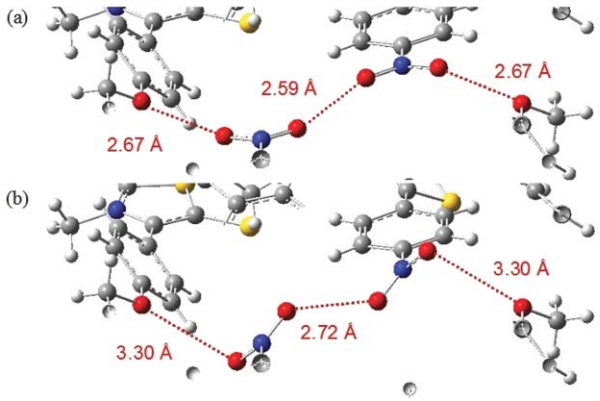

Fig. 3 Intermolecular interactions involving the oxygen atoms of nitro and methoxy groups in a hypothetical supramolecular structure having the 4-nitrophenyl groups in coplanar disposition (a) and the real aggregate with twisted 4-nitrophenyl groups (b).

Furthermore, to assess the ability of DFT calculations to reproduce the crystal lattice of **25**, the two 4-nitrophenyl groups depicted in Fig. 2 have been optimized freezing the Cartesian coordinates of the remaining atoms (thus preserving the unit cell). Such an optimization leads to a structure with a dihedral angle O–N–C–C of 37.7°, which closely matches the situation found experimentally (40.5°).

Unlike **20**, the reactions of münchnones **21–23** with carbon disulfide resulted in formation of a single product (**26–28**, respectively) whose structures were assigned on the basis of their ^{1}H and ^{13}C NMR data. Quantitative elemental analysis further confirmed the existence of two sulfur atoms. Suitable crystals for X-ray diffraction could be obtained for compound **28**, thereby revealing the *meta* substitution of the nitrophenyl group.

Mechanistic Insights

The 1,3-dipolar cycloaddition of 1,3-oxazolium-5-olates with carbon disulfide should be a concerted reaction controlled by the symmetry of the frontier orbitals of the reactants. Two possible orientations (Scheme 3, *a* or *b*) may be envisaged. The first pathway (*a*) would involve binding of the C-4 carbon atom of the heterocycle to the thiocarbonyl group of carbon disulfide to form cycloadducts **30–33**. Had the reaction proceeded by route *b*, the C-2 carbon would become attached to the thiocarbonyl carbon, thus yielding cycloadducts **34–37**. Both pathways would afford, after the elimination of carbon dioxide, the expected 1,3-thiazolium-5-thiolate systems, although the new heterocycles would differ in the relative positions of substituents R^1 and R^2 relative to the endocyclic and exocyclic sulfur atoms. This accounts for the formation of a mixture (compounds **24** and **25**) starting from münchnone **20**.

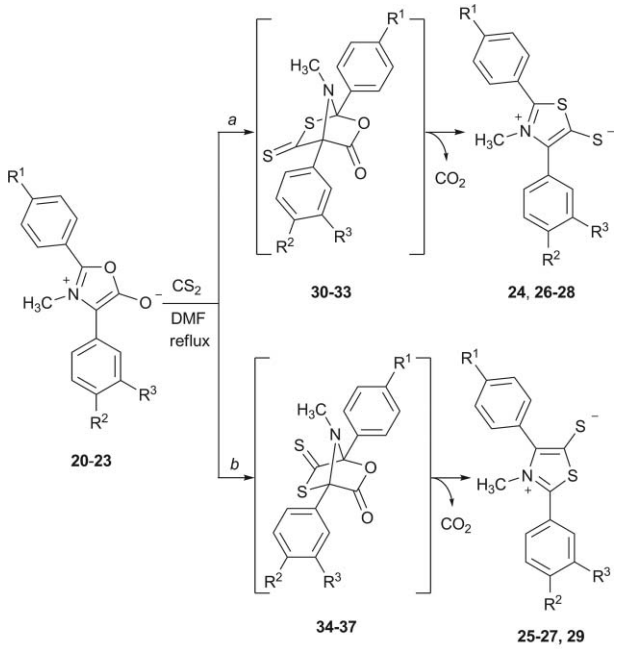

20, 24, 25, 30, 34 $R^1 = NO_2$; $R^2 = OCH_3$; $R^3 = H$
21, 26, 27, 31, 35 $R^1 = F$; $R^2 = OCH_3$; $R^3 = H$
22, 32, 36 $R^1 = OCH_3$; $R^2 = F$; $R^3 = H$
23, 28, 29, 33, 37 $R^1 = OCH_3$; $R^2 = H$; $R^3 = NO_2$

Scheme 3

The frontier orbital energies of both reactants, calculated at the B3LYP/6-31G(d) level, evidence that the reaction of münchnones with carbon disulfide should be classed as a Sustmann type I cycloaddition controlled by the interaction HOMO (dipole)-LUMO (dipolarophile), whose coefficients in the reaction centers explain the formation of thiolates **24** and **26–28**, derived from the initial cicloadducts **30–33** (pathway *a*). However, the similarity of the c_2 and c_4 coefficients of the HOMOs in compounds **20–23** does not rule out the possible formation of cycloadducts **34–37** (pathway *b*) in some cases (Table 2). This hypothesis is corroborated by the lack of regioselectivity observed experimentally in the cycloaddition of **20**.

To shed light into the origin of the regioselectivity pattern, we have optimized, at the same level of theory, the structures of all stationary states involved in the two possible approaches of carbon disulfide to münchnones **20–23**. Table 3 shows the relative free energies of these structures, which almost fully agree with experimental results; *i.e.* preferred or exclusive isolation of

Table 2 Frontier orbital energies and coefficients of münchnones **20–23** and carbon disulfide calculated at the B3LYP/6-31G(d) level

Substrate	MO	Energy/eV	c_2	c_4	c_S	c_C
20	HO	−5.00445	−0.27	0.30		
	LU	−2.83815	0.30	0.18		
21	HO	−4.51517	−0.26	0.27		
	LU	−1.65760	0.32	0.18		
22	HO	−4.55312	−0.25	0.29		
	LU	−1.54943	0.34	0.16		
23	HO	−4.95868	−0.24	0.30		
	LU	−1.81377	0.35	0.14		
S_2C	HO	−7.55857			0.52	0.00
	LU	−2.03896			−0.36	0.49

Table 3 Relative free energies (in kcal mol^{-1}), calculated at the B3LYP/6-31G(d) level, for all stationary states involved in the cycloadditions of münchnones **20–23** with carbon disulfide

Reactants	Pathway	Saddle Point	Intermediate	Saddle Point	Cycloadduct	Products
20 + S_2C (0.00)	*a*	$\mathbf{SP}_{20\rightarrow30}$ (34.00)	—	—	**30** (25.24)	**24** + CO_2 (–9.67)
	b	$\mathbf{SP}_{20\rightarrow34}$ (32.60)	—	—	**34** (22.40)	**25** + CO_2 (–11.50)
21 + S_2C (0.00)	*a*	$\mathbf{SP}_{21\rightarrow31}$ (30.34)	—	—	**31** (23.35)	**26** + CO_2 (–10.43)
	b	$\mathbf{SP}_{21\rightarrow35}$ (31.68)	—	—	**35** (21.17)	**27** + CO_2 (–11.27)
22 + S_2C (0.00)	*a*	$\mathbf{SP1}_{22\rightarrow32}$ (30.32)	$\mathbf{I}_{22\rightarrow32}$ (29.70)	$\mathbf{SP2}_{22\rightarrow32}$ (31.08)	**32** (24.03)	**27** + CO_2 (–9.90)
	b	$\mathbf{SP}_{22\rightarrow36}$ (33.83)	—	—	**36** (22.85)	**26** + CO_2 (–9.06)
23 + S_2C (0.00)	*a*	$\mathbf{SP}_{23\rightarrow33}$ (33.32)	—	—	**33** (26.55)	**28** + CO_2 (–8.64)
	b	$\mathbf{SP}_{23\rightarrow37}$ (37.87)	—	—	**37** (26.07)	**29** + CO_2 (–5.82)

regioisomers whose formation is kinetically favored. However, they do not justify the formation of a single product from münchnone **21**, since the free energies of the two regioisomeric transition structures ($SP_{21\rightarrow31}$ and $SP_{21\rightarrow35}$) only differ by 1.34 kcal mol^{-1}.

The polar nature of the transition structures suggests that solvent effects might also play a key role. To evaluate this influence the transition structures $SP_{21\rightarrow31}$ and $SP_{21\rightarrow35}$ have been optimized in DMF at the B3LYP/6-31G(d) level using the CPCM model and UAKS cavities. This solvent effect correction indicates that $SP_{21\rightarrow31}$ increases its stability with respect to $SP_{21\rightarrow35}$ up to 3.92 kcal mol^{-1} (Fig. 4).

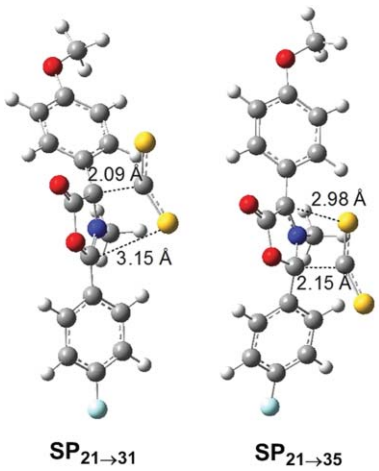

Fig. 4 Transition structures $SP_{21\rightarrow31}$ and $SP_{21\rightarrow35}$ optimized in DMF at the B3LYP/6-31G(d) level using the CPCM model and UAKS cavities.

The location of a single saddle point for the reactions of **20**, **21** and **23** shows that, regardless of the chosen approach, these processes are concerted. The exception to this behavior was found in the reaction of **22**, for which two transition structures ($SP1_{22\rightarrow32}$ and $SP2_{22\rightarrow32}$) along with a dipolar intermediate ($I_{22\rightarrow32}$) could be located for the energetically favored pathway *a* (Fig. 5) relative to the concerted route *b* ($\Delta\Delta G^{\neq} = 2.75$ kcal mol^{-1}).

This result suggests that strong electron-withdrawing groups attached to the C-4 carbon atom of the heterocycle switch a concerted 1,3-dipolar cycloaddition mechanism into a two-step process, which evolves through a high-energy dipolar intermediate. To confirm this point still further, we have also studied the hypothetical reaction of the 4-nitrophenyl-substituted münchnone (**38**) with carbon disulfide. In this case the theoretical calculations

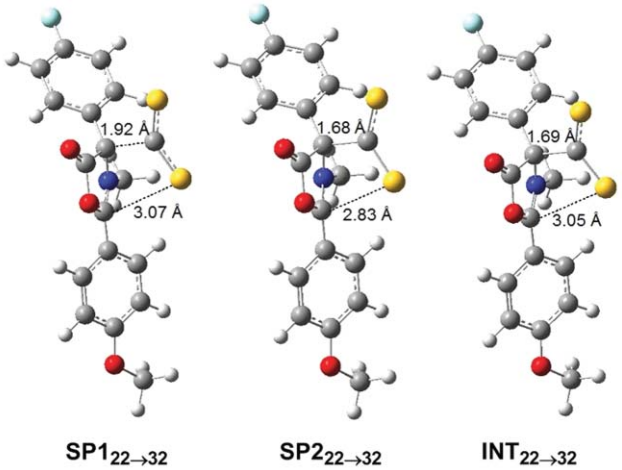

Fig. 5 Transition structures $SP1_{22\rightarrow32}$ and $SP2_{22\rightarrow32}$ and the dipolar intermediate $I_{22\rightarrow32}$.

also located a dipolar intermediate and two saddle points (Fig. 6), with an energy barrier of 34.8 kcal mol^{-1}.

Electronic and Electrochemical data

Electronic absorption spectra of compounds **24–28** showed an intense broad band associated with a one-electron HOMO→LUMO transition (Fig. 7), which was also calculated at the B3LYP/6-31G(d) level (Table 4).

The cyclic voltammograms of **24–28** displayed both one irreversible oxidation wave and one irreversible reduction wave, regardless of the position and nature of the aryl groups linked to C-2 and C-4 atoms of the heterocyclic moiety. The presence

Table 4 Physical properties of compounds **24–28**

	Electronic data		Electrochemical data[d]	
Comp.	λ_{max}/nm[a]	λ_{max}/nm[b] [f][c]	Oxidation E^0/V	Reduction E^0/V
24	535	669 [0.37]	0.71	–0.11
25	436	620 [0.22]	0.71	–0.10
26	452	529 [0.27]	0.68	–0.23
27	448	519 [0.27]	0.62	–0.20
28	443	517 [0.19]	0.72	–0.17

[a] In DMSO. [b] At B3LYP/6-31G(d) level (vacuum). [c] Oscillator strength. [d] Potentials recorded *vs.* Ag/AgCl in 0.1 M trioctylmethylammonium chloride (Adogen 464)/DMSO, using a glassy carbon working electrode and a Pt counter electrode, at 20 °C, with a scan rate of 50 mV s^{-1}

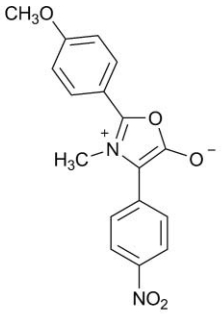

38

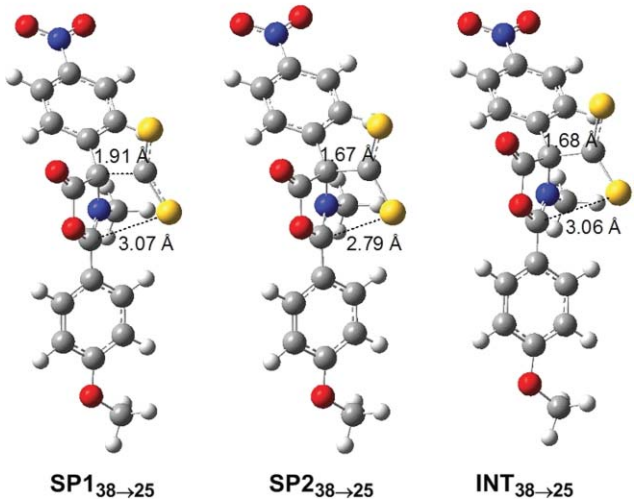

Fig. 6 Transition structures and dipolar intermediate located for the hypothetical reaction of **38** and CS_2.

of a nitro group (compounds **24**, **25**, and **28**) shifts slightly the E_{ox} values toward more anodic potentials and the E_{red} toward less cathodic potentials than does a fluorine atom (compounds **26** and **27**). This trend is mirrored by theoretical calculations, which showed that the nitro group decreases both the E_{HOMO} and E_{LUMO} values (Table 5).

Nonlinear Optical Properties

The second-order NLO properties of compounds **24–28** were estimated by calculating their molecular hyperpolarizabilities using the coupled perturbed Hartree–Fock (CPHF), the finite-field (FF), and the time-dependent Hartree–Fock (TDHF) methods implemented at the GAUSSIAN03[7] and GAMESS[8] software packages.

To establish the appropriate level of theory, we performed a preliminary calculation of the $\beta(0)_{tot}$ values for 4-nitroaniline

Table 5 Frontier orbital energies (eV) for compounds **24–28** calculated at the B3LYP/6-31+G(d) level

Compound	E_{HOMO}	E_{LUMO}	$\Delta E_{HOMO-LUMO}$
24	–5.27	–3.37	1.90
25	–5.20	–2.82	2.38
26	–4.84	–2.24	2.60
27	–4.83	–2.12	2.71
28	–5.11	–2.83	2.28

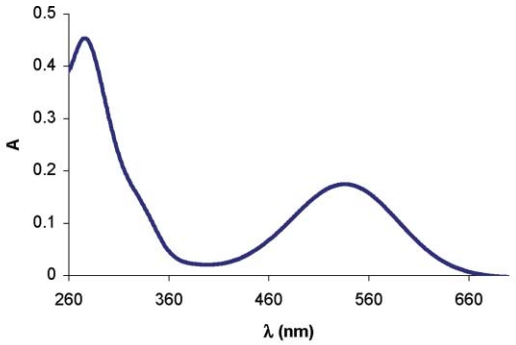

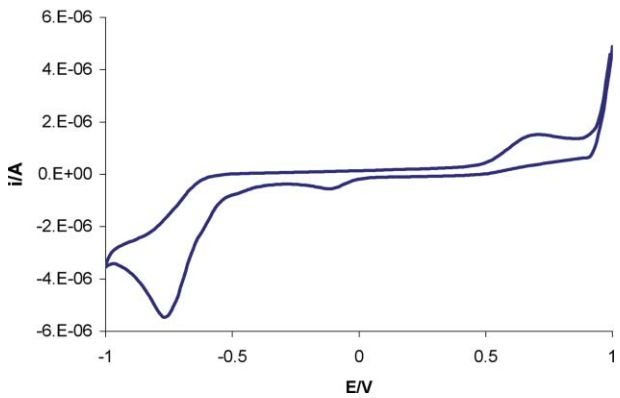

Fig. 7 (a) Absorption spectra of **24** in DMSO. (b) Cyclic voltammogram of **24** in 0.1 M trioctylmethylammonium chloride (Adogen 464)/DMSO, $v = 50$ mV s^{-1}.

(pNA) and *N*,*N*-dimethylaminonitrostilbene (DANS) (Table 6) whose experimental $\beta(0)$ values have been determined to be 17×10^{-30} and 55×10^{-30} esu, respectively.[9]

The $\beta(0)_{tot}$ values collected in Table 6 reproduce reasonably well the experimental results when using diffuse basis sets irrespective of the level (HF or B3LYP) used for calculation. Therefore, the theoretical calculation of the hyperpolarizabilities of the 1,3-thiazolium-5-thiolates **24–28** was carried out using the FF method at the B3LYP/6-31+G(d) level, whereas both TDHF and CPHF methods were conducted at the HF/6-31+G(d) level. Data thus obtained (Table 7) showed that compound **24** had higher hyperpolarizabilities than pNA and DANS, while mesoionics **25–28** showed values higher than those reported for pNA but lower than those of DANS.

Furthermore, a closer analysis of the structure-property relationship suggests that the hyperpolarizability acquires higher values when the 1,3-thiazolium-5-thiolate system possesses an

Table 6 $\beta(0)_{tot}$ values ($\times 10^{-30}$ esu) calculated for pNA and DANS through the FF, TDHF, and CPHF methods

Basis set	FF (B3LYP)		TDHF (HF)		CPHF (HF)	
	pNA	DANS	pNA	DANS	pNA	DANS
6-31G(d)	11.44	210.61	16.44	203.53	6.83	69.15
6-31+G(d)	14.87	260.94	15.72	196.88	8.01	78.38
6-311G(d)	11.45	216.67	15.97	207.94	6.72	70.61
6-311G(d,p)	11.34	217.19	15.69	208.50	6.62	70.87
6-311+G(d)	14.61	259.31	15.84	206.65	7.95	78.66
6-311+G(d,p)	14.49	259.73	15.54	207.12	7.84	78.93

Table 7 $\beta(0)_{tot}$ and $\beta(\omega)_{tot}$[a] values (in 10^{-30} esu) calculated for compounds **24–28** through the FF[b], TDHF[c], and CPHF[c] methods

	FF	TDHF		CPHF	
Compound	$\beta(0)_{tot}$	$\beta(0)_{tot}$	$\beta(\omega)_{tot}$	$\beta(0)_{tot}$	$\beta(\omega)_{tot}$
24	286.79	380.96	527.74	134.39	188.51
25	98.65	62.93	79.11	17.01	20.07
26	55.16	122.68	157.41	39.00	49.93
27	30.65	93.13	118.99	25.72	33.27
28	21.24	68.44	87.76	16.21	21.86

[a] $\omega = 1064$ nm. [b] At B3LYP/6-31+G(d) level. [c] At HF/6-31+G(d) level.

electron-withdrawing group attached to C-2 and an electron-releasing group on the C-5 atom; a structural situation encountered in compounds **24** and **26**. The effect caused by a fluorine atom is significantly lower than that produced by the nitro group at the same position.

A further inspection of the frontier orbitals in compounds **24–28** reveals that their HOMOs are mainly located over the C4═C5–S- heterocyclic framework while the corresponding LUMO topologies are determined by the position and electronic nature of aryl groups linked to the C-2 and C-4 atoms. Thus, the LUMO of **24** largely concentrates on the 4-$NO_2C_6H_4$-C2 group and the pictures of both frontier orbitals (Fig. 8, left) make it possible to imagine the charge transfer taking place between such orbitals when the material is stimulated with a strong electric field. This charge transfer, in which the C-2 carbon atom act as the overlapping path of transition, will induce a change in the polarization that is oriented in the direction of the electron-attracting group (4-nitrophenyl); in fact a necessary condition for a large nonlinear response to occur.[10] However, the LUMO of **25** is very spread along the aryl groups attached to C-2 and C-4 (Fig. 8, right). Accordingly, when this material is coupled with a strong electric field, its polarization will be reduced due to partial cancellation of contributions directed toward the 4-nitrophenyl and 4-methoxyphenyl groups. As a result, compound **25** does not behave like a typical push-pull system in which both sides (nucleophilic and electrophilic) are clearly differentiated.

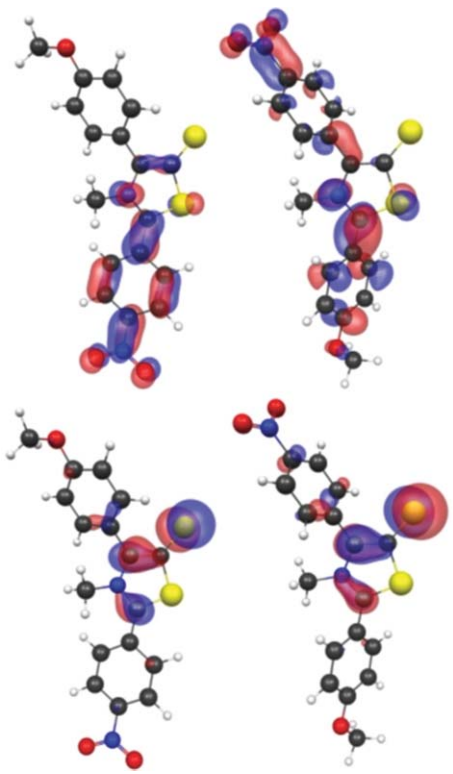

Fig. 8 Calculated orbital topologies (B3LYP/6-31G(d) level) for the HOMOs (below) and the LUMOs (above) of **24** (left) and **25** (right).

The energy difference between HOMO and LUMO orbitals should equally be checked in the search for molecular candidates with nonlinear optical responses. It is generally accepted that there is an inverse relationship between the first hyperpolarizability and the HOMO–LUMO energy gap, thereby enabling the overlap of orbitals and charge transfers from the donor to acceptor groups. As inferred from Table 5, the HOMO–LUMO energy gaps (in eV) calculated at the B3LYP/6-31+G(d) for compounds **24–28**, are similar to the value found for DANS (2.76 eV) and lower than that of pNA (4.14 eV), two push-pull molecules which have good nonlinear responses.

Conclusions

Condensations of 1,3-oxazolium-5-olates with carbon disulfide in refluxing DMF yield the corresponding thiazolium-5-thiolates in moderate to good yields. Compounds **21–23** afford a single product, while two regioisomeric substances are isolated in the case of münchnone **20**, and whose structures and particular crystal packing have been elucidated by X-ray crystallography.

A mechanistic analysis conducted at the B3LYP/6-31G(d) level suggests two possible reaction channels for the dipolar cycloaddition to occur. Gas-phase calculations do satisfactorily predict the experimental results, while solvent effects appear to be important in the case of compound **21**, for which only a correction using the CPCM model explains the observed regioselectivity. While most reactions follow a concerted pathway, the presence of a strong electron-withdrawing group at the C-4 atom (*e.g.* **22**) triggers a stepwise reaction for which the dipolar intermediate and saddle points have been determined.

Compounds **24–28** exhibit intense electronic absorptions in the visible range and undergo irreversible redox processes. Computation of hyperpolarizabilities and orbital geometries evidences that these push-pull 1,3-thiazolium-5-thiolates show promising perspectives as a novel family of molecules with NLO responses. Further experimental and theoretical studies in this context are currently under way.

Experimental Section

N-methyl-*C*-phenylglycine hydrochloride (11)

Following the described procedure[6] compound **11** was obtained (62%); mp 231–233 °C, ^{1}H NMR (400 MHz, DMSO-d_6) 10.02 (sa, 2H), 7.59–3.34 (m, 5H), 5.07 (s, 1H), 2.38 (s, 3H).

C-(4-Methoxyphenyl)-*N*-methylglycine hydrochloride (12)

Following the described procedure[6] compound **12** was obtained (42%); mp 227–229 °C, ^{1}H NMR (400 MHz, DMSO-d_6) 10.07 (sa, 1H), 9.63 (sa, 1H), 7.45 (d, *J* 8.8 Hz, 2H), 7.01 (d, *J* 8.8 Hz, 2H), 4.99 (s, 1H), 3.76 (s, 3H)

C-(4-Fluorophenyl)-*N*-methylglycine hydrochloride (13)

To a solution of 4-fluorobenzaldehyde (4.9 g, 39.1 mmol) in methanol (8 mL) was added a solution of sodium cyanide (1.9 g, 39,4 mmol) and methyl ammonium chloride (3.0 g, 44,4 mmol) in water (8 mL). The mixture was stirred at room temperature for 4 h, then diluted with water (20 mL), and extracted with benzene (3 × 7 mL). The organic phase was extracted again with HCl 6*M* (3 × 8 mL), the aqueous layer was separated and heated at reflux for 10 h. The solution was cooled to room temperature, and the resulting crystals were filtered and washed with CCl_4 (3.7 g, 43%); mp 198–199 °C; ^{1}H NMR (400 MHz, DMSO-d_6): 9.99 (sa, 2H), 7.61 (dd, *J* 8.0 Hz, *J* 5.2 Hz, 2H), 7.33 (t, *J* 8.8 Hz, 2H), 5.14 (s, 1H), 2.39 (s, 3H); ^{13}C NMR (100 MHz, DMSO-d_6) 169.4, 163.2, 131.7, 127.9, 116.6, 62.5, 31.0; IR (KBr, cm^{-1}) 3500, 2500, 1744, 836. Anal. Calcd for $C_9H_{11}ClFNO_2$: C, 49.22; H, 5.05; N, 6.38. Found: C, 49.49; H, 5.15; N, 6.46.

C-(3-Nitrophenyl)-*N*-methylglycine hydrogen sulfate (15)

Following the procedure reported for the synthesis of *C*-(4-nitrophenyl)-*N*-methylglycine hydrogen sulfate (**14**),[6] compound **15** was obtained (78%); mp 163–165 °C; ^{1}H NMR (400 MHz, DMSO-d_6) 8.43 (s, 1H), 8.33 (d, *J* 6.0 Hz, 1H), 7.94 (d, *J* 6.8 Hz, 1H), 7.81 (t, *J* 7.6 Hz, 1H), 5.33 (s, 1H), 2.51 (s, 3H); ^{13}C NMR (100 MHz, DMSO-d_6) 169.0, 148.5, 135.9, 133.7, 131.4, 125.2, 124.1, 62.8, 31.6.

C-(4-Methoxyphenyl)-*N*-methyl-*N*-(4-nitrobenzoyl)glycine (16)

Following the described procedure,[6] compound **16** was obtained (42%); mp 148–149 °C; ^{1}H NMR (400 MHz, DMSO-d_6) 8.22–6.89 (m, 8H), 5.96 (s, 1H), 3.68 (s, 3H), 2.50 (s, 3H).

C-(4-Fluorophenyl)-*N*-(4-methoxybenzoyl)-*N*-methylglycine (18)

To a solution of **13** (3.0 g, 13.7 mmol) and NaOH (1.6 g, 40.3 mmol) in water (24 mL) was added dropwise 4-methoxybenzoyl chloride (2.14 g, 12.5 mmol). The reaction mixture was stirred for 4 h, and then HCl 12*M* (3.5 mL) was added. The resulting solid was filtered off and washed with water (76%); mp 57–58 °C; ^{1}H NMR (400 MHz, DMSO-d_6) 7.42–6.99 (m, 8H), 5.99 (sa, 1H), 3.80 (s, 3H), 2.73 (s, 3H); ^{13}C NMR (100 MHz, DMSO-d_6) 171.5, 167.5, 162.3, 160.9, 131.8, 131.5, 129.7, 128.1, 123.4, 116.0, 114.2, 61.1, 55.7, 35.8; IR (KBr, cm^{-1}) 3500, 2500, 1729, 1688. Anal. Calcd for $C_{17}H_{16}FNO_4$: C, 64.35; H, 5.08; N, 4.41. Found: C, 64.51; H, 5.35; N, 4.53.

N-(4-Methoxybenzoyl)-*N*-methyl-*C*-(3-nitrophenyl)glycine (19)

Following the procedure reported for the synthesis of *N*-(4-methoxybenzoyl)-*N*-methyl-*C*-(4-nitrophenyl)glycine,[6] compound **19** was obtained (36%). ^{1}H NMR (400 MHz, DMSO-d_6) 8.42 (s, 1H), 8.33 (d, *J* 8.4 Hz, 1H), 8.03 (d, *J* 8.4 Hz, 1H), 7.82 (t, *J* 8.0 Hz, 1H), 7.55 (d, *J* 8.4 Hz, 2H), 7.07 (d, *J* 8.4 Hz, 2H), 6.25 (sa, 1H), 3.88 (s, 3H), 2.84 (s, 3H).

2-(4-Nitrophenyl)-4-(4-methoxyphenyl)-3-methyl-1,3-oxazolium-5-olate (20)

Following the described procedure[6] compound **20** was obtained (42%); mp 190–192 °C, ^{1}H NMR (400 MHz, DMSO-d_6) 8.37 (d, *J* 9.2 Hz, 2H), 7.98 (d, *J* 9.2 Hz, 2H), 7.47 (d, *J* 8.8 Hz, 2H), 7.04 (d, *J* 8.8 Hz, 2H), 3.91 (s, 3H), 3.80 (s, 3H).

2-(4-Fluorophenyl)-4-(4-methoxyphenyl)-3-methyl-1,3-oxazolium-5-olate (21)

A suspension of **18** (3 mmol) in acetic anhydride (5 mL) was stirred under argon atmosphere at 55 °C. When the substrate was completely dissolved the solvent was removed under vacuum. The resulting solid was filtered off and washed with ethyl ether (37%); mp 134–135 °C, ^{1}H NMR (400 MHz, DMSO-d_6) 7.84 (ddd, *J* 7.2 Hz, *J* 5.2 Hz, *J* 2.4 Hz, 2H), 7.47 (t, *J* 8.8 Hz, 2H), 7.43 (d, *J* 8.8 Hz, 2H), 7.01 (d, *J* 8.8 Hz, 2H), 3.79 (s, 3H), 3.78 (s, 3H); ^{13}C NMR (100 MHz, DMSO-d_6): 163.6, 160.0, 157.7, 141.5, 131.0, 121.9, 120.1, 117.0, 114.6, 95.4, 55.6, 36.5; IR (KBr, cm^{-1}) 1689. Anal. Calcd for $C_{17}H_{14}FNO_3$: C, 68.22; H, 4.71; N, 4.68. Found: C, 68.50; H, 4.78; N, 4.81.

4-(4-Fluorophenyl)-2-(4-methoxyphenyl)-3-methyl-1,3-oxazolium-5-olate (22)

To a solution of **12** (3.0 g, 12.9 mmol) and NaOH (1.61 g, 40.3 mmol) in water (24 mL) was added dropwise 4-fluorobenzoyl chloride (1.98 g, 12.5 mmol). The reaction mixture was stirred for 4 h, and then HCl 12M (3.5 mL) was added. The resulting oil was extracted with CH_2Cl_2 and the organic phase dried with Na_2SO_4. Then, the solvent was evaporated and the residue treated with acetic anhydride under argon, and stirred at 55 °C until it was completely dissolved. The solvent was evaporated and the solid filtered off and washed with ethyl ether (20%); mp 158–159 °C; ^{1}H NMR (400 MHz, DMSO-d_6) 7.75 (d, *J* 8.8 Hz, 2H), 7.54 (dd, *J* 8.8 Hz, *J* 2.8 Hz, 2H), 7.24 (t, *J* 8.8 Hz 2H), 7.18 (d, *J* 8.8 Hz, 2H), 3.87 (s, 3H), 3.34 (s, 3H); ^{13}C NMR (100 MHz, DMSO-d_6) 161.8, 159.8, 144.0, 130.5, 128.4, 128.3, 126.6, 126.6, 115.9, 115.7, 115.4, 115.3, 94.1, 56.1, 36.8; IR (KBr, cm^{-1}) 1685. Anal. Calcd for $C_{17}H_{14}FNO_3$: C, 68.22; H, 4.71; N, 4.68. Found: C, 67.90; H, 4.88; N, 4.72.

2-(4-Methoxyphenyl)-3-methyl-4-(3-nitrophenyl)-1,3-oxazolium-5-olate (23)

Following the procedure reported for the synthesis of 2-(4-methoxyphenyl)-3-methyl-4-(4-nitrophenyl)-1,3-oxazolium-5-olate,[6] compound **23** was similary obtained (49%), ^{1}H NMR (400 MHz, DMSO-d_6) 8.42 (t, *J* 2.0 Hz, 1H), 7.95 (d, *J* 8.0 Hz, 1H), 7.91 (dd, *J* 8.0 Hz, *J* 1.6 Hz, 1H), 7.80 (d, *J* 8.8 Hz, 2H), 7.65 (t, *J* 8.0 Hz, 1H), 7.20 (d, *J* 9.2, 1H), 3.93 (s, 3H), 3.88 (s, 3H).

General Procedure for the Preparation of 1,3-Thiazolium-5-thiolate Systems

A mixture of the münchnone (**20–23**) (1 mmol) and CS_2 (1 mL) in DMF (3 mL) was heated at reflux. The reaction mixture was monitored by TLC (benzene–acetonitrile 2 : 1) until the complete disappearance of the parent mesoionic ring (1–4 h). Then, it was

purified by flash chromatography (benzene–acetonitrile gradient elution from 5 : 1 to 1 : 5).

4-(4-Methoxyphenyl)-3-methyl-2-(4-nitrophenyl)-1,3-thiazolium-5-thiolate (24). 34%; mp 213–214 °C; ^{1}H NMR (400 MHz, DMSO-d_6) 8.41 (d, *J* 8.8 Hz, 2H), 8.02 (d, *J* 8.8 Hz, 2H), 7.55 (d, *J* 8.8 Hz, 2H), 7.10 (d, *J* 8.8 Hz, 2H), 3.83 (s, 3H), 3.65 (s, 3H); ^{13}C NMR (100 MHz, DMSO-d_6) 162.0, 160.0, 149.1, 148.8, 141.7, 133.4, 133.1, 131.4, 128.8, 124.8, 122.7, 114.4, 55.7, 41.7; IR (KBr, cm^{-1}) 1607, 1593, 1523, 1351. Anal. Calcd for $C_{17}H_{14}N_2O_3S_2$: C, 56.96; H, 3.94; N, 7.82; S, 17.89. Found: C, 56.67; H, 3.87; N, 8.04; S, 18.01.

2-(4-Methoxyphenyl)-3-methyl-4-(4-nitrophenyl)-1,3-thiazolium-5-thiolate (25). 43%; mp 216–217 °C; ^{1}H NMR (400 MHz, DMSO-d_6) 8.37 (d, J 8.8 Hz, 2H), 8.01 (d, J 8.8 Hz, 2H), 7.73 (d, J 8.8 Hz, 2H), 7.20 (d, J 8.8 Hz, 2H), 3.87 (s, 3H), 3.67 (s, 3H); ^{13}C NMR (100 MHz, DMSO-d_6) 162.4, 156.7, 147.0, 137.8, 137.7, 132.6, 132.0, 128.8, 123.8, 119.2, 115.4, 56.2, 41.9; IR (KBr, cm^{-1}) 1605, 1592, 1508, 1338. Anal. Calcd for $C_{17}H_{14}N_2O_3S_2$: C, 56.96; H, 3.94; N, 7.82; S, 17.89. Found: C, 56.68; H, 3.95; N, 8.02; S, 18.13.

2-(4-Fluorophenyl)-4-(4-methoxyphenyl)-3-methyl-1,3-thiazolium -5-thiolate (26). 61%; mp 244–245 °C; ^{1}H NMR (400 MHz, DMSO-d_6) 7.81 (ddd, J 8.8 Hz, J 2.0 Hz, J 1.2 Hz, 2H), 7.53 (d, J 8.4 Hz, 2H), 7.48 (t, J 8.4 Hz, 2H), 7.09 (d, J 8.4 Hz, 2H), 3.83 (s, 3H) 3.57 (s, 3H); ^{13}C NMR (100 MHz, DMSO-d_6) 162.8, 159.8, 159.7, 152.0, 140.2, 133.0, 132.8, 132.7, 124.1, 123.1, 117.2, 117.0, 114.3, 55.7, 41.2; IR (KBr, cm^{-1}) 1606, 1597. Anal. calcd for $C_{17}H_{14}FNOS_2$: C, 61.61; H, 4.26; N, 4.23; S, 19.35. Found: C, 60.89; H, 3.98; N, 4.49; S, 19.50.

4-(4-Fluorophenyl)-2-(4-methoxyphenyl)-3-methyl-1,3-thiazolium-5-thiolate (27). This compound crystallized from the reaction medium after heating for 1h. The solid was filtered and washed with diethyl ether (98%); mp 204–205 °C; ^{1}H NMR (400 MHz, DMSO-d_6) 7.69 (m, 4H), 7.36 (t, *J* 8.8 Hz, 2H), 7.18 (d, *J* 8.8 Hz, 2H), 3.86 (s, 3H), 3.60 (s, 3H); ^{13}C NMR (100 MHz, DMSO-d_6) 162.4, 162.1, 159.1, 154.6, 138.8, 134.0, 131.8, 127.6, 119.5, 115.8, 115.4, 56.1, 41.4; IR (KBr, cm^{-1}) 1604, 1498. Anal. calcd for $C_{17}H_{14}FNOS_2$: C, 61.61; H, 4.26; N, 4.23; S, 19.35. Found: C, 61.33; H, 3.94; N, 4.36; S, 19.42.

2-(4-Methoxyphenyl)-3-methyl-4-(3-nitrophenyl)-1,3-thiazolium-5-thiolate (28). 36%; mp 192–193 °C; ^{1}H NMR (400 MHz, DMSO-d_6) 8.61 (s, 1H), 8.27 (dd, *J* 8.0 Hz, *J* 2.0 Hz 1H), 8.11 (d, *J* 7.6 Hz, 1H), 8.01 (t, *J* 8.0 Hz, 1H), 7.72 (d, *J* 8.8 Hz, 2H), 7.18 (d, *J* 8.8 Hz, 2H), 3.86 (s, 3H), 3.66 (s, 3H); ^{13}C NMR (100 MHz, DMSO-d_6) 162.3, 159.9, 156.0, 148.1, 138.2, 137.5, 132.6, 131.9, 130.3, 126.5, 123.5, 119.2, 115.4, 56.1, 41.7. IR (*ν*, KBr): 1602, 1568, 1525, 1346. Anal. calcd for $C_{17}H_{14}N_2O_3S_2$: C, 56.96; H, 3.94; N, 7.82; S, 17.89. Found: C, 56.92; H, 3.83; N, 7.94; S, 18.20.

Acknowledgements

The Spanish Ministry of Education and Science (CTQ2007-66641/BQU) and FEDER, and the Junta de Extremadura (PRI07-A016) have supported financially this investigation. Special thanks go to Ara Cantillo for her bibliographical assistance. We are also grateful to the Ministry of Education and Science for a grant to D.C.

References

1 (*a*) R. Huisgen, E. Funke, F. C. Schaefer, H. Gotthardt and E. Brunn, *Tetrahedron Lett.*, 1967, **8**, 1809; (*b*) E. Funke, R. Huisgen and F. C. Schaefer, *Chem. Ber.*, 1971, **104**, 1550.
2 K. Potts, in *1,3-Dipolar Cycloaddition Chemistry*, A. Padwa, Ed.; Wiley: New York, 1984, Vol. 2, p. 1.
3 (*a*) G. L. C. Moura, A. M. Simas and J. Miller, *Chem. Phys. Lett.*, 1996, **257**, 639; (*b*) P. F. Athayde-Filho, J. Miller, A. M. Simas, B. F. Lira, J. A. S. Luis and J. Zuckerman-Schpector, *Synthesis*, 2003, 685; (*c*) A. M. S. Silva, G. B. Rocha, P. H. Menezes, J. Miller and A. M. Simas, *J. Braz. Chem. Soc.*, 2005, **16**, 583; (*d*) B. F. Lyra, S. A. Morais, G. B. Rocha, J. Miller, G. L. C. Moura, A. M. Simas, C. Peppe and P. F. Athayde-Filho, *J. Braz. Chem. Soc.*, 2010, **21**, 934.
4 D. Cantillo, M. Ávalos, R. Babiano, P. Cintas, J. L. Jiménez, M. E. Light and J. C. Palacios, *J. Org. Chem.*, 2009, **74**, 7644.
5 (*a*) D. Cantillo, M. Ávalos, R. Babiano, P. Cintas, J. L. Jiménez, M. E. Light and J. C. Palacios, *Org. Lett.*, 2008, **10**, 1079; (*b*) D. Cantillo, M. Ávalos, R. Babiano, P. Cintas, J. L. Jiménez, M. E. Light and J. C. Palacios, *J. Org. Chem.*, 2009, **74**, 3698.
6 H. O. Bayer, R. Huisgen, R. Knorr and F. C. Schaefer, *Chem. Ber.*, 1970, **103**, 2581.
7 Gaussian 03, *Revision C.02*, M. J. Frisch, G. W. Trucks, H. B. Schlegel, G. E. Scuseria, M. A. Robb, J. R. Cheeseman, J. A. Montgomery, Jr., T. Vreven, K. N. Kudin, J. C. Burant, J. M. Millam, S. S. Iyengar, J. Tomasi, V. Barone, B. Mennucci, M. Cossi, G. Scalmani, N. Rega, G. A. Petersson, H. Nakatsuji, M. Hada, M. Ehara, K. Toyota, R. Fukuda, J. Hasegawa, M. Ishida, T. Nakajima, Y. Honda, O. Kitao, H. Nakai, M. Klene, X. Li, J. E. Knox, H. P. Hratchian, J. B. Cross, V. Bakken, C. Adamo, J. Jaramillo, R. Gomperts, R. E. Stratmann, O. Yazyev, A. J. Austin, R. Cammi, C. Pomelli, J. W. Ochterski, P. Y. Ayala, K. Morokuma, G. A. Voth, P. Salvador, J. J. Dannenberg, V. G. Zakrzewski, S. Dapprich, A. D. Daniels, M. C. Strain, O. Farkas, D. K. Malick, A. D. Rabuck, K. Raghavachari, J. B. Foresman, J. V. Ortiz, Q. Cui, A. G. Baboul, S. Clifford, J. Cioslowski, B. B. Stefanov, G. Liu, A. Liashenko, P. Piskorz, I. Komaromi, R. L. Martin, D. J. Fox, T. Keith, M. A. Al-Laham, C. Y. Peng, A. Nanayakkara, M. Challacombe, P. M. W. Gill, B. Johnson, W. Chen, M. W. Wong, C. Gonzalez, and J. A. Pople, Gaussian, Inc., Wallingford CT, 2004.
8 (*a*) M. W. Schmidt, K. K. Baldridge, J. A. Boatz, S. T. Elbert, M. S. Gordon, J. H. Jensen, S. Koseki, N. Matsunaga, K. A. Nguyen, S. J. Su, T. L. Windus, M. Dupuis and J. A. Montgomery, *J. Comput. Chem.*, 1993, **14**, 1347; (*b*) M. S. Gordon, and M. W. Schmidt, "Advances in Electronic Structure Theory: GAMESS A Decade Later" in *"Theory and Applications of Computational Chemistry, The First Forty Years"*, ed.: C. E. Dykstra, G. Frenking, K. S. Kim, and G. E. Scuseria, Elsevier, Amsterdam, 2005, Cap. 41, p. 1167.
9 P. J. A. Kenis, E. G. Kerver, B. H. M. Snellink-Ruel, G. J. Hummel van, S. Harkema, M. C. Flipse, R. H. Woudenberg, J. F. J. Engbersen and D. N. Reinhoudt, *Eur. J. Org. Chem.*, 1998, 1089.
10 (*a*) D. R. Kanis, M. A. Ratner and T. J. Marks, *Chem. Rev.*, 1994, **94**, 195; (*b*) T. Vijayakumar, I. H. Joe, C. P. R. Nair and V. S. Jayakumar, Proceedings of the 2nd International Conference on Perspectives in Vibrational Spectroscopy (ICOPVS 2008), *AIP Conf. Proc.*, 2008, **1075**, 85.

